The Multipole Expansion of the Local Expansion Rate

Basheer Kalbouneh

Centre de Physique Théorique
Aix-Marseille Université

In collaboration with: Christian Marinoni & Julien Bel

arXiv:2210.11333

Colloque national Action Dark Energy 2022 - 6ème édition (17/11/2022)

Introduction

The Standard Model of Cosmology

- The standard cosmological model relies on the theory of general relativity, with the cosmological principle (CP), which states that the universe is spatially homogeneous and isotropic.

- In the standard model of cosmology, all the cosmological parameters (density parameters Ω, Hubble parameter H …) depend only on time.

- Hubble constant tension problem is one of the main problems in standard cosmology.

In the local universe:

$$H_0 = 73.2 \pm 1.3\, km/s/Mpc$$

(Riess et al. 2021)

By CMB:

$$H_0 = 67.4 \pm 0.5\, km/s/Mpc$$

(Planck Collaboration et al. 2020)

Introduction

- One of the possible solution for Hubble constant tension is that the local universe is not homogeneous and isotropic.

- Traditionally, deviations from CP predictions are treated perturbatively by expanding the cosmological parameters into a smooth background component and a fluctuating part.

- We developed a completely non-perturbative and model-independent approach to investigate the local inhomogeneities.

The Expansion Rate Fluctuations

- In any generic spacetime (metric), for small redshift (z<<1) (natural units c = 1),

$$z = \tilde{H}_0(\theta, \phi) d$$

- We defined a new variable (η):

$$\eta(\theta, \phi) \equiv \log\left[\frac{\tilde{H}_0(\theta, \phi)}{H_0}\right]$$

- For each object, (η) is estimated by the distance modulus

$$\hat{\eta} = \log\left[\frac{z}{H_0}\right] + 5 - \frac{\mu}{5}$$

- The estimator is independent from H_0, and is a Gaussian random variable and statistically unbiased.

- The physical interpretation in the FRW cosmological model (if radial peculiar velocity v<<z)

$$\eta \approx \frac{v}{z \ln 10}$$

The Expansion Rate Fluctuations

- By using **HEALPix** (Hierarchical Equal Area isoLatitude Pixelisation of a 2-sphere).

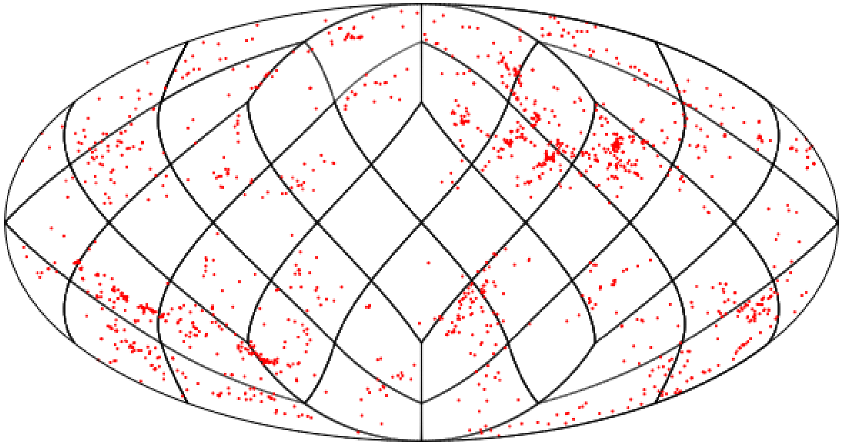

Number of pixels = 48

The Expansion Rate Fluctuations

- ❑ By using **HEALPix** (Hierarchical Equal Area isoLatitude Pixelisation of a 2-sphere).

- ❑ Rotation to handle angular incompleteness.

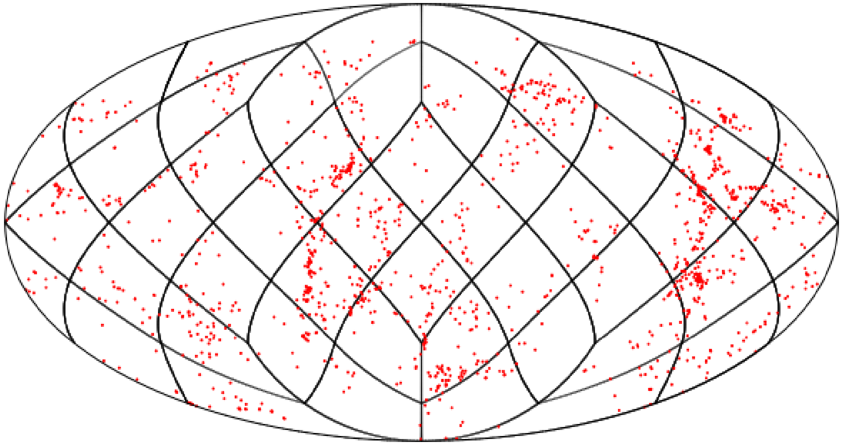

Number of pixels = 48

The Expansion Rate Fluctuations

- By using **HEALPix** (Hierarchical Equal Area isoLatitude Pixelisation of a 2-sphere).

- Rotation to handle angular incompleteness.

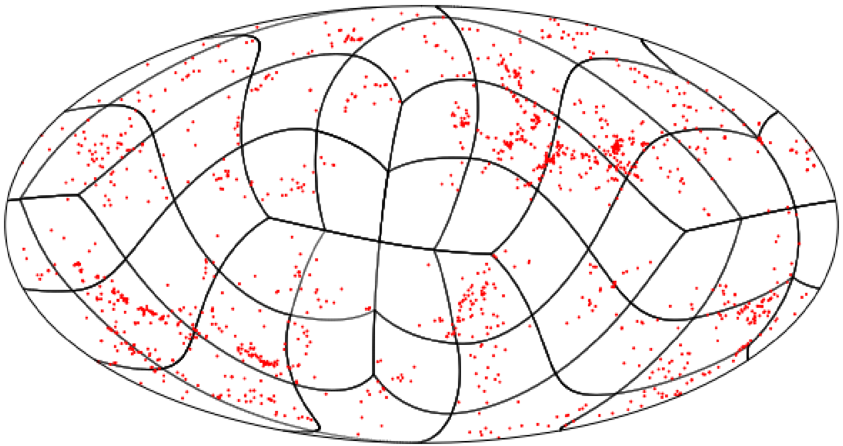

Number of pixels = 48

The Expansion Rate Fluctuations

- By using **HEALPix** (Hierarchical Equal Area isoLatitude Pixelisation of a 2-sphere).

- Rotation to handle angular incompleteness.

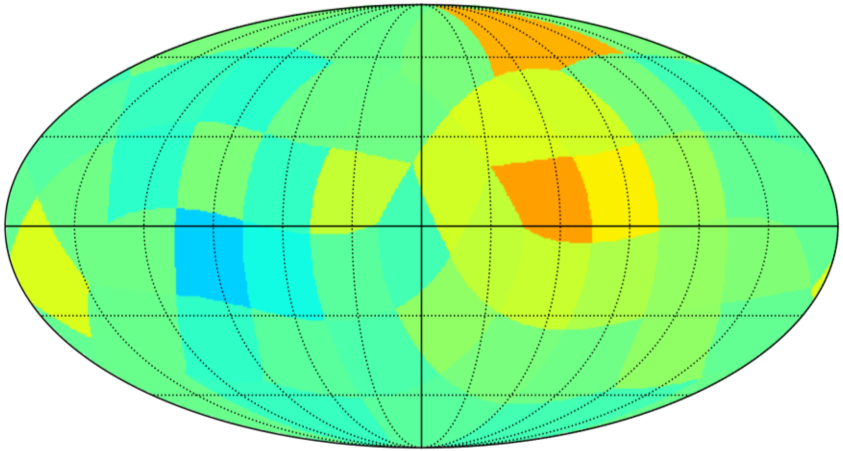

- Define a piece-wise function.

$$\eta(\Omega) = \left\langle \log\left[\frac{\tilde{H}_0}{H_0}\right]\right\rangle_{\Omega}$$

- It is then decomposed into the spherical harmonic basis

$$\eta = \sum_{\ell=0}^{\infty}\sum_{m=-\ell}^{\ell} a_{\ell m} Y_{\ell m}(\theta, \phi)$$

The Expansion Rate Fluctuations

- The spherical harmonic coefficients

$$a_{\ell m} \equiv \int_0^{2\pi} \int_0^{\pi} \eta(\theta,\phi) Y^*_{\ell m}(\theta,\phi) \sin\theta \, d\theta d\phi$$

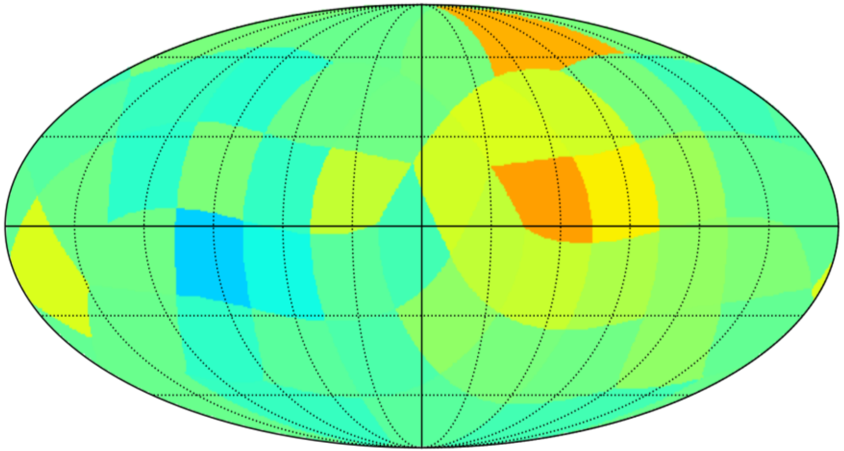

- The zeroth order estimator is

$$\hat{a}^{(0)}_{\ell m} = \frac{4\pi}{N_{pix}} \sum_{p=1}^{N_{pix}} \eta(\Omega_p) Y^*_{\ell m}(\theta_p,\phi_p)$$

- The higher order estimator is

$$\hat{a}^{(k+1)}_{\ell m} = \hat{a}^{(k)}_{\ell m} + \frac{4\pi}{N_{pix}} \sum_{p=1}^{N_{pix}} \Big(\eta(\Omega_p) - \eta^{(k)}(\theta_p,\phi_p)\Big) Y^*_{\ell m}(\theta_p,\phi_p) \quad , \quad \eta^{(k)}(\theta_p,\phi_p) = \sum_{\ell=0}^{\ell_{max}} \sum_{m=-\ell}^{\ell} \hat{a}^{(k)}_{\ell m} Y_{\ell m}(\theta_p,\phi_p)$$

- The power spectrum $\hat{C}_\ell = \frac{1}{2\ell+1} \sum_{m=-\ell}^{\ell} |a^{(\infty)}_{\ell m}|^2$

Data

1) **Pantheon** SNIa sample (Scolnic et al. 2018)

- Almost isotropic for z < 0.05 with (158 objects).
- The typical error in the distance modulus ($\boldsymbol{\Delta\mu = 0.15}$).

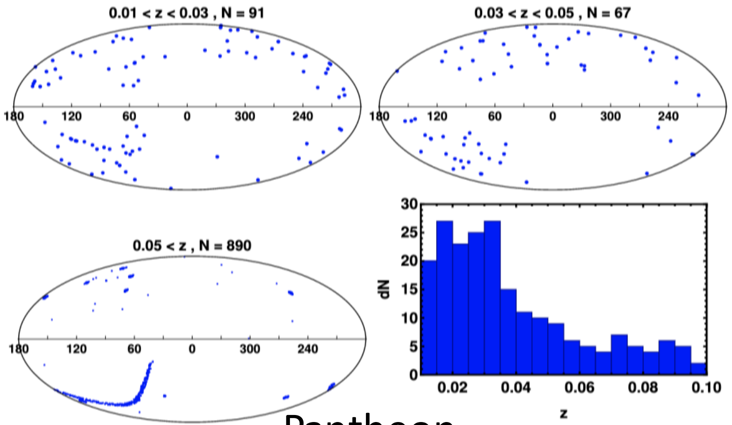

Pantheon

2) **Cosmic-Flows 3 (CF3)** galaxies (Tully et al. 2017)

- Almost isotropic for z < 0.05 with (13661 objects).
- We divided the sample into two independent subsamples:

A) **CF3 SNIa**: 286 objects ($\boldsymbol{\Delta\mu = 0.18}$).

B) **CF3 galaxies**: 13375 objects ($\boldsymbol{\Delta\mu = 0.46}$).

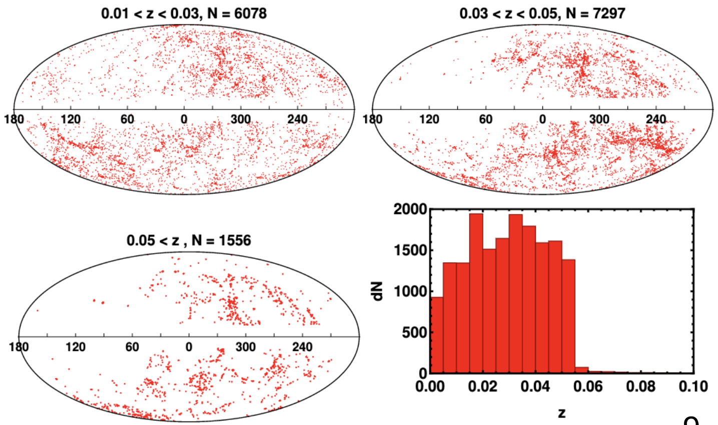

Cosmic-Flows 3

Results

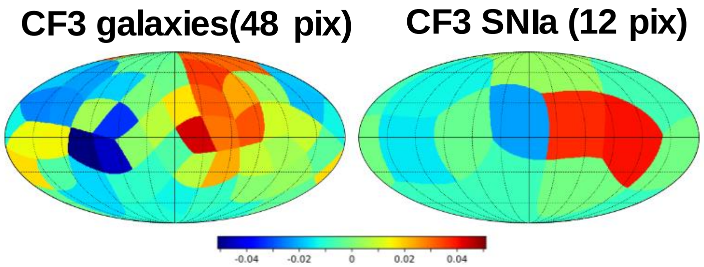

η maps

Results

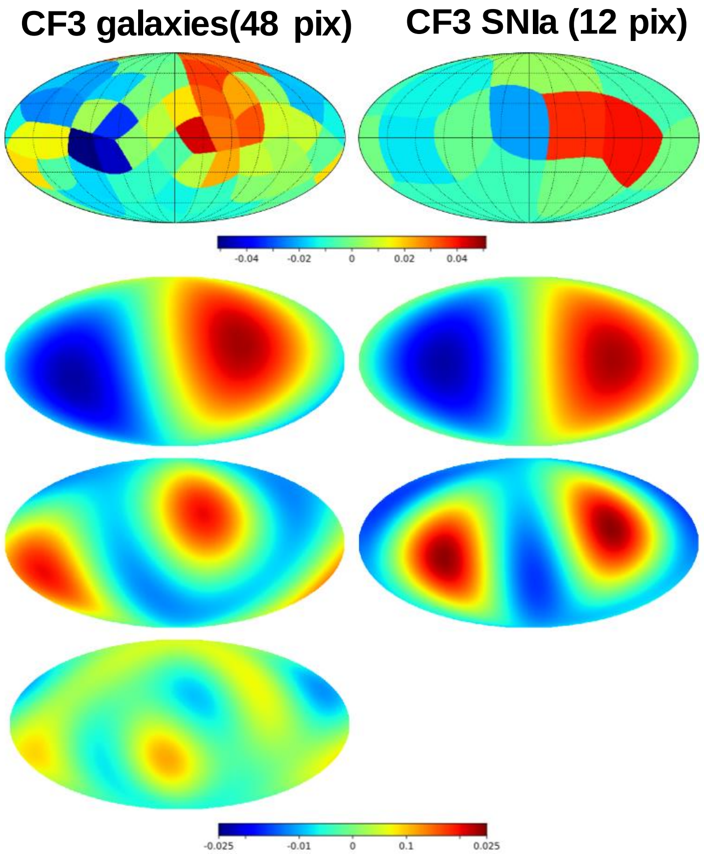

η maps

Same intensity and direction (CF3g, CF3sn and Pantheon).
Signal 2% of monopole.
Same direction as bulk component of LG motion.

Results

CF3 galaxies(48 pix) **CF3 SNIa (12 pix)**

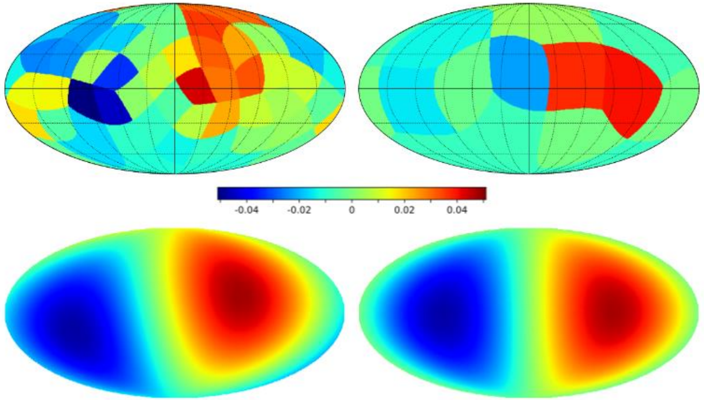

η maps

Same intensity and direction (CF3g, CF3sn and Pantheon).
Signal 2% of monopole.
Same direction as bulk component of LG motion.

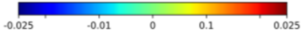

Results

CF3 galaxies(48 pix) CF3 SNIa (12 pix)

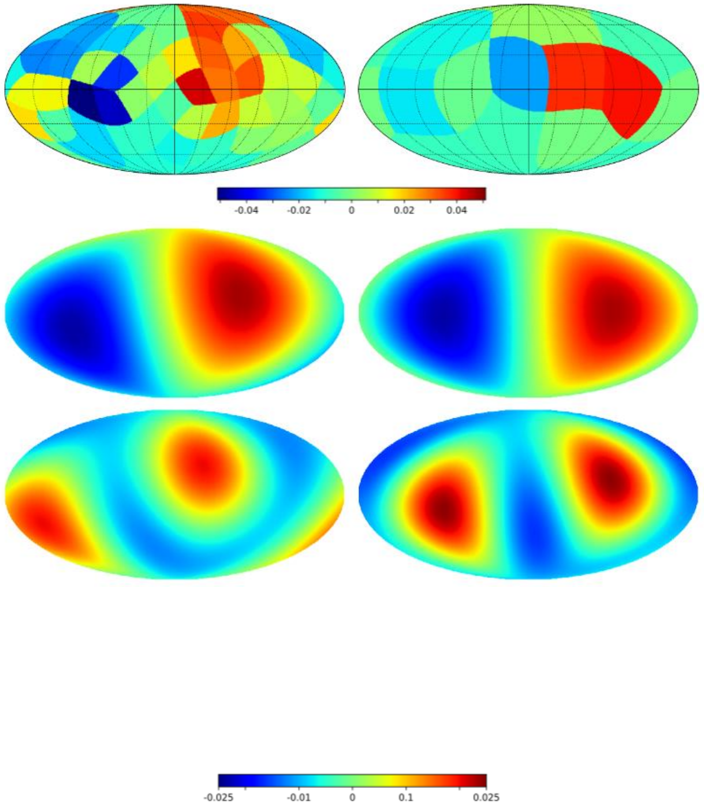

η maps

Same intensity and direction (CF3g, CF3sn and Pantheon).
Signal 2% of monopole.
Same direction as bulk component of LG motion.

Quadrupole intensity is half that of the dipole
Alignement with the direction of the dipole
No quadrupole component in Pantheon data!

Results

CF3 galaxies(48 pix)   CF3 SNIa (12 pix)

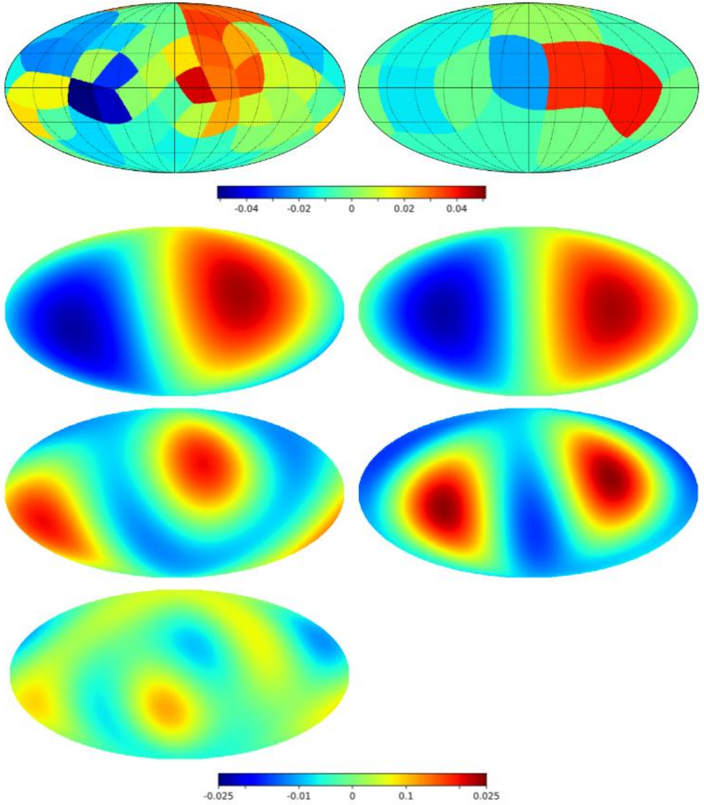

η maps

Same intensity and direction (CF3g, CF3sn and Pantheon).
Signal 2% of monopole.
Same direction as bulk component of LG motion.

Quadrupole intensity is half that of the dipole
Alignement with the direction of the dipole
No quadrupole component in Pantheon data!

Octupole: only for CF3 the S/N is acceptable (~3.1)

Results

CF3 galaxies(48 pix) **CF3 SNIa (12 pix)**

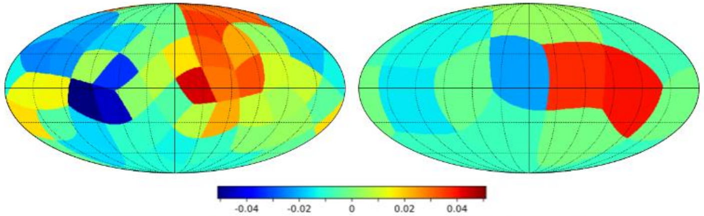

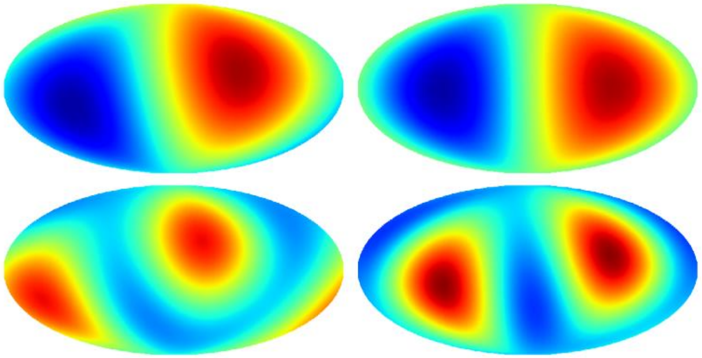

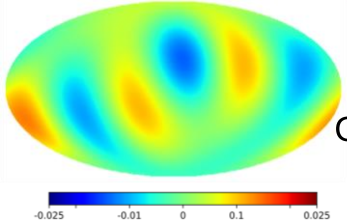

Octupole of full CF3 sample

η maps

Same intensity and direction (CF3g, CF3sn and Pantheon).
Signal 2% of monopole.
Same direction as bulk component of LG motion.

Quadrupole intensity is half that of the dipole.
Alignement with the direction of the dipole.
No quadrupole component in Pantheon data.

Octopole: only for CF3 the S/N is acceptable (~3.1)

The Robustness of the Results

- ❑ Independent from pixelisation strategy.

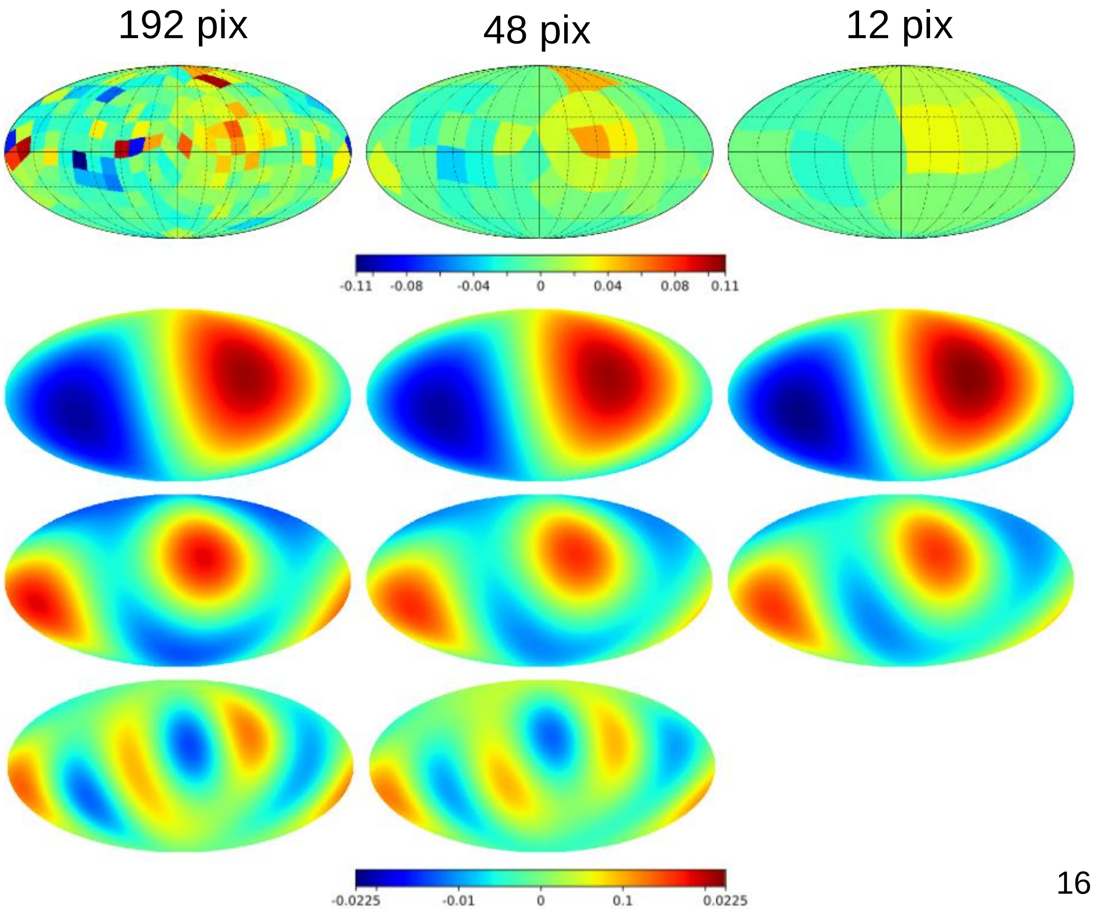

The Robustness of the Results

- Independent from pixelisation strategy.
- Independent from the sample depth.

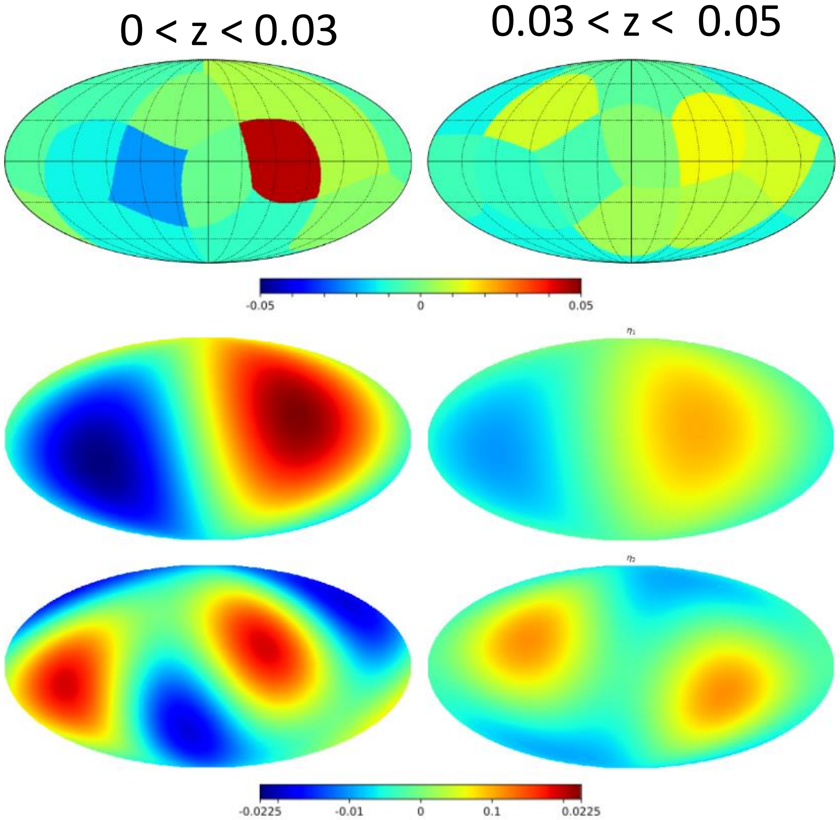

The Robustness of the Results

- Independent from pixelisation strategy.

- Independent from the sample depth.

- Consistent with results of fitting the data with the spherical harmonics.

	Fourier	Fit	Fourier	Fit	Fourier	Fit	Fourier	Fit
Sample	l_d		b_d		$C_1/10^4$		$C_2/10^4$	
CF3 [0.01, 0.05]	285 ± 5	287 ± 5	11 ± 4	10 ± 4	5.1 ± 0.8	4.3 ± 0.8	1 ± 0.3	1.2 ± 0.3
CF3g [0.01, 0.05]	296 ± 6	290 ± 5	18 ± 5	5 ± 4	4.0 ± 0.6	5.3 ± 0.9	1.3 ± 0.4	1.3 ± 0.3
CF3sn [0.01, 0.05]	322 ± 23	293 ± 14	−8 ± 18	0 ± 10	3.7 ± 1.5	5.5 ± 2.6	1.7 ± 1.4	1.8 ± 1.1
Pantheon [0.01, 0.05]	332 ± 39	312 ± 23	−9 ± 19	19 ± 26	3.9 ± 2.7	3.4 ± 3.2	0.5 ± 1.4	0.6 ± 1.0

Errors and Biases

- The errors and biases are computed by 1000 Monte Carlo simulations.

- Variance of the power spectrum coefficients

$$\boxed{V\left[\hat{C}_\ell\right] = \left(\frac{1}{2\ell+1}\right)^2 \sum_{n=0}^{2\ell} V[w_n^{(\ell)}]}$$

where

$$V[w_n^{(\ell)}] = \begin{cases} 2\sigma_{\ell 0}^4 + 4\sigma_{\ell 0}^2 a_{\ell 0}^2 & n = 0 \\ 8\sigma_{\ell n}^{(R)4} + 16\sigma_{\ell n}^{(R)2}\Re[a_{\ell n}]^2 & \ell \geq n > 0 \\ 8\sigma_{\ell(n-\ell)}^{(I)4} + 16\sigma_{\ell(n-\ell)}^{(I)2}\Im[a_{\ell(n-\ell)}]^2 & 2l \geq n > \ell \end{cases}$$

and $\sigma_{\ell m}^{(R)2} = V[\Re[\hat{a}_{\ell m}]]$, $\sigma_{\ell m}^{(I)2} = V[\Im[\hat{a}_{\ell m}]]$

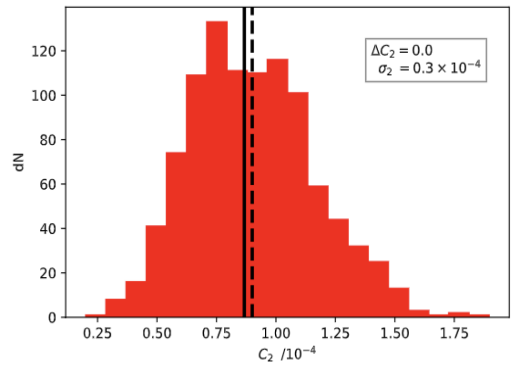

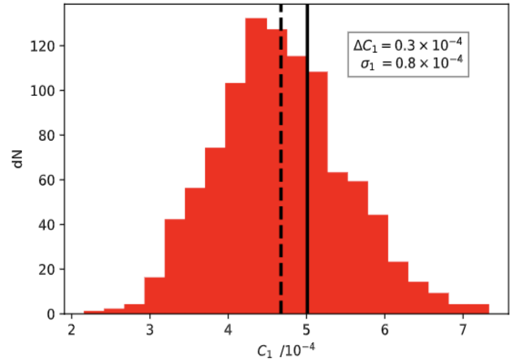

Axial Symmetry

- 3D structure of the quadrupole (Galactic plane shown for reference)

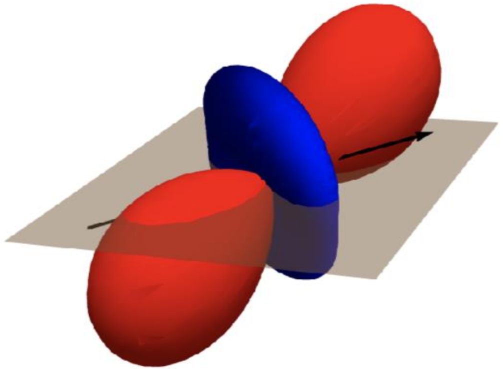

CF3 Galaxies

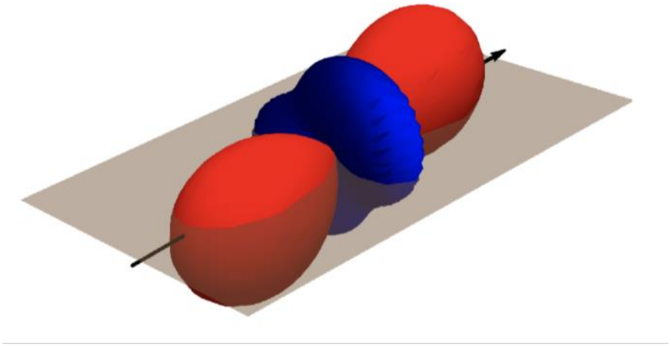

CF3 SNIa

- The quadrupole is symmetric around the axis of the maximum ($l \sim 285$, $b \sim 11$).

Axial Symmetry

- Sufficient to expand using the Legendre basis about the axis of symmetry

$$\eta(\alpha) = \sum_{\ell=1}^{\infty} a_\ell P_\ell(\cos\alpha)$$

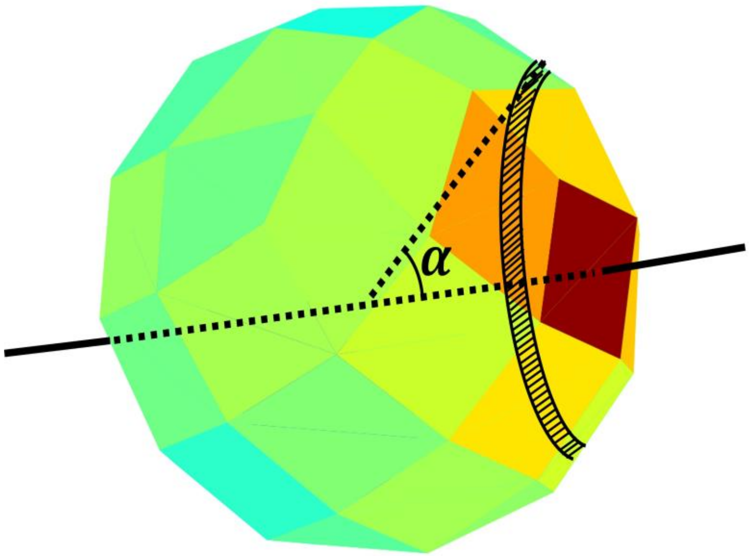

Axial Symmetry

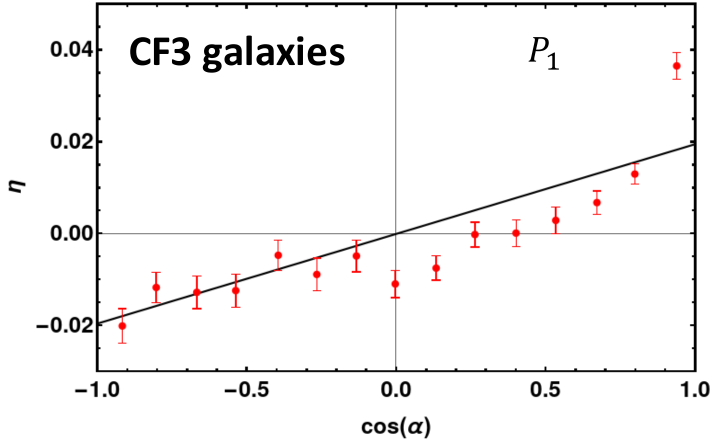

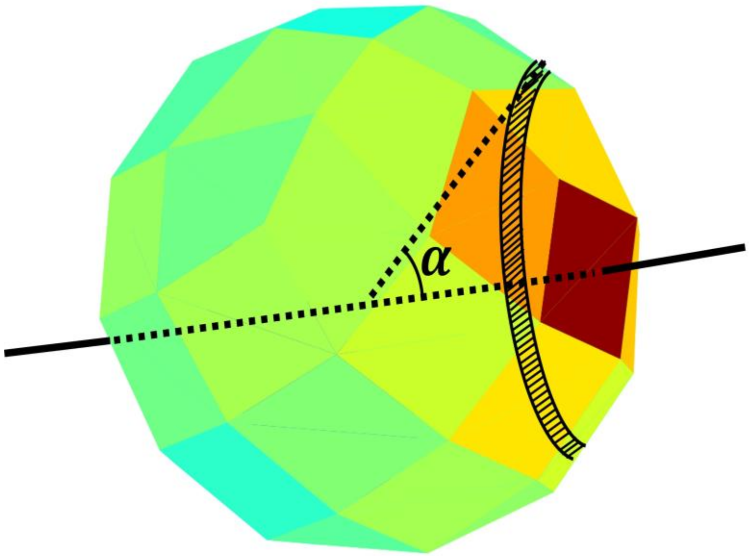

Axial Symmetry

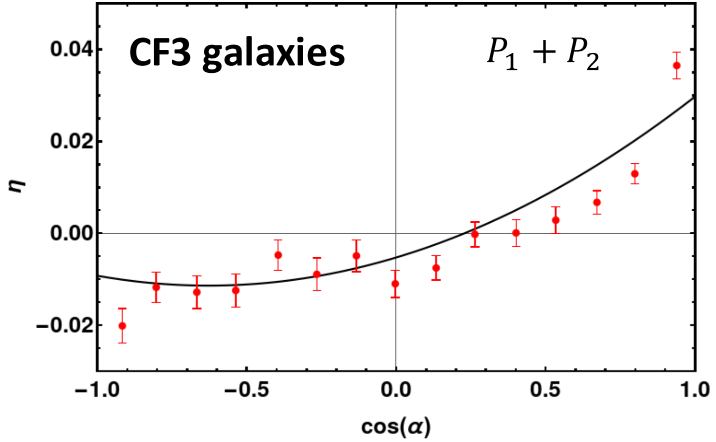

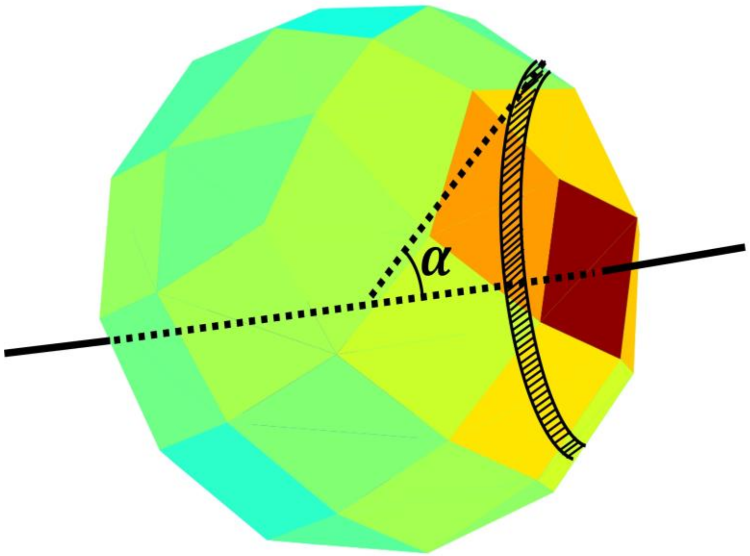

Axial Symmetry

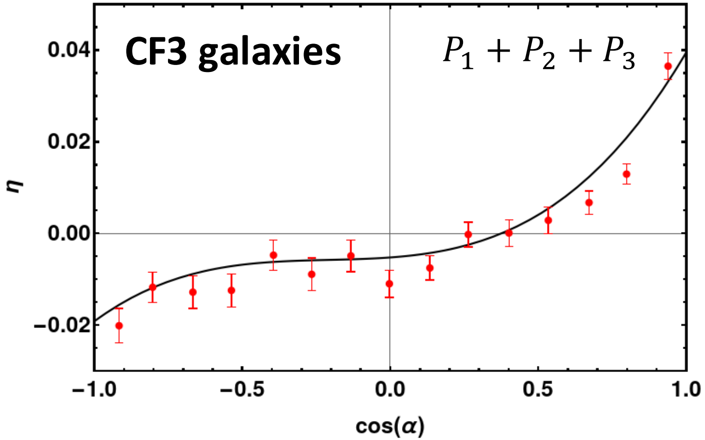

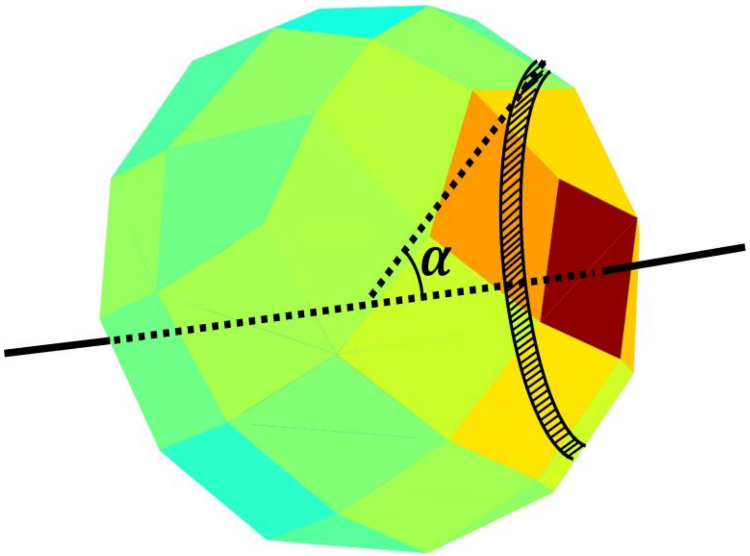

Axial Symmetry

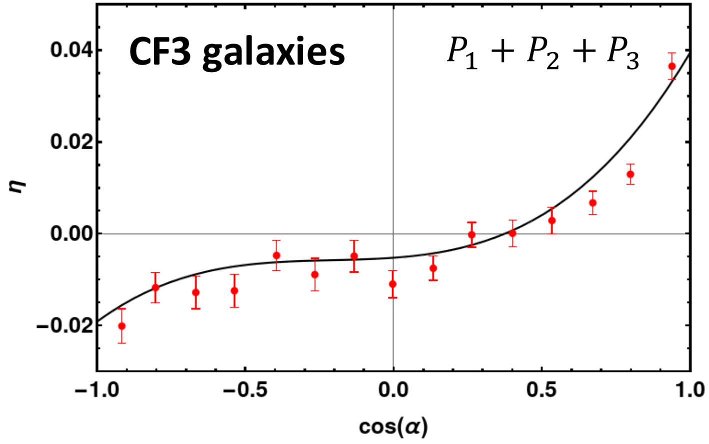

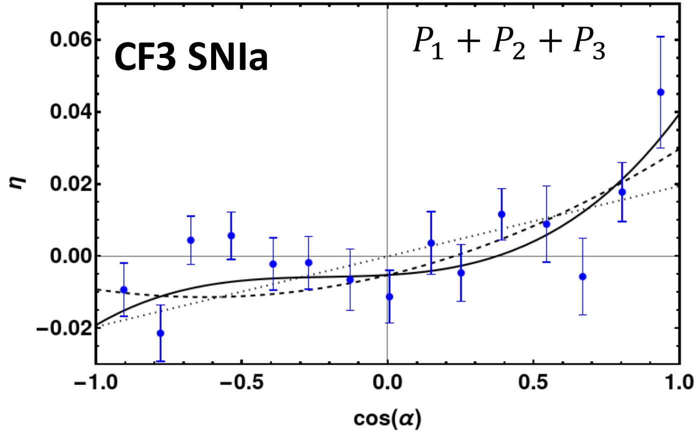

- The same 3 Legendre coefficients can describe the measurements for both samples.

$$a_1 = (1.9 \pm 0.1) \times 10^{-2}$$
$$a_2 = (1.1 \pm 0.1) \times 10^{-2}$$
$$a_3 = (1.1 \pm 0.1) \times 10^{-2}$$

Axial Symmetry

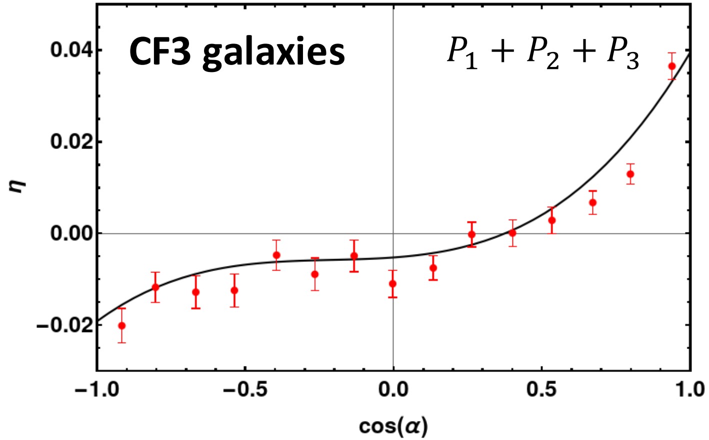

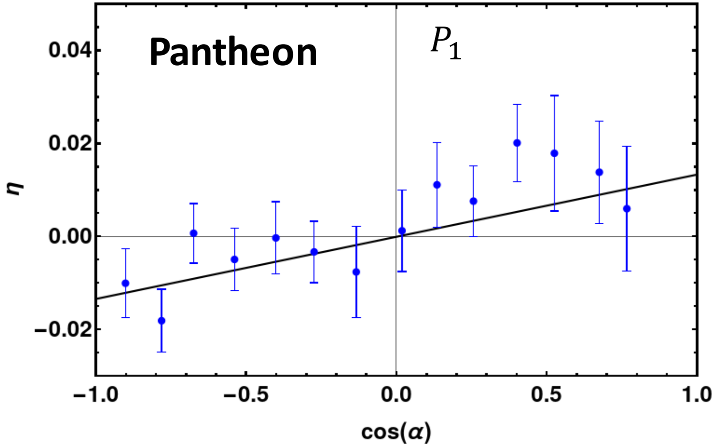

- The same 3 Legendre coefficients can describe the measurements for both samples.

$$a_1 = (1.9 \pm 0.1) \times 10^{-2}$$
$$a_2 = (1.1 \pm 0.1) \times 10^{-2}$$
$$a_3 = (1.1 \pm 0.1) \times 10^{-2}$$

- For Pantheon sample, the dipole is enough, since the error is larger (due to the small number of objects), and there is no objects in the interesting direction.

Axial Symmetry: bulk motion

- The bulk velocity is related to the dipole.

$$v_b = \frac{a_1 \ln 10}{\langle (1+z)/z \rangle} \qquad = 318 \pm 22 \text{ km/s}$$

$$v_b = 252 \pm 11 \text{ km/s}$$

(S. S. Boruah, M. J. Hudson, and G. Lavaux. 2020)

$$v_b = 292 \pm 28 \text{ km/s}$$

(T. Hong et al. 2014)

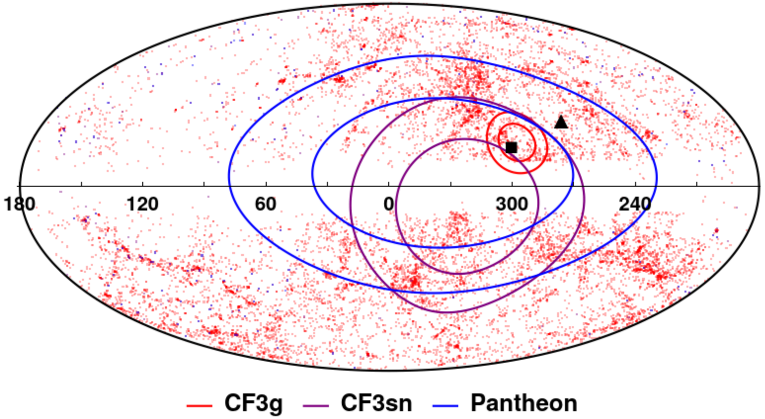

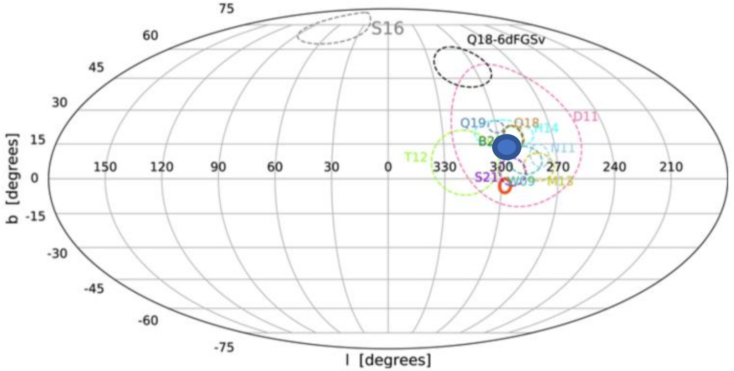

(Qin et al. 2021)

Bulk flow direction

Axial Symmetry: peculiar velocity

- Since (η) is related to the radial peculiar velocity.

$$\mu = 5\log\left(\frac{z}{H_0}\right) + 25 - 5\eta$$

The map of the signal-to-noise ratio for ΔH_0, between each direction and its opposite direction

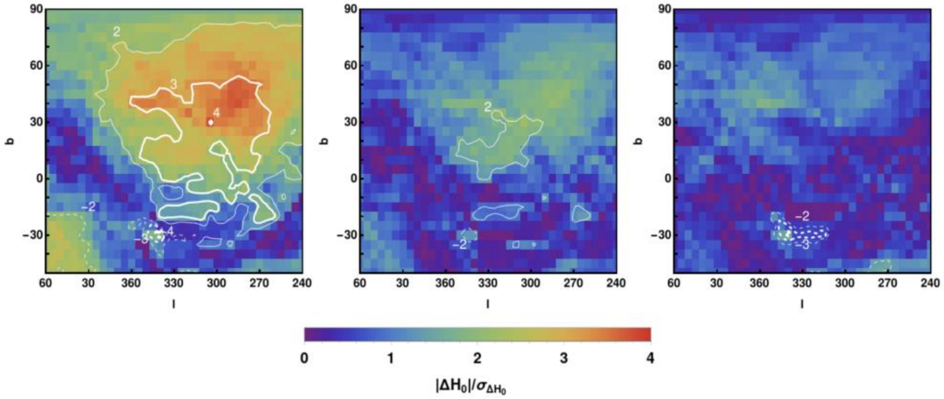

The dipole of Pantheon sample

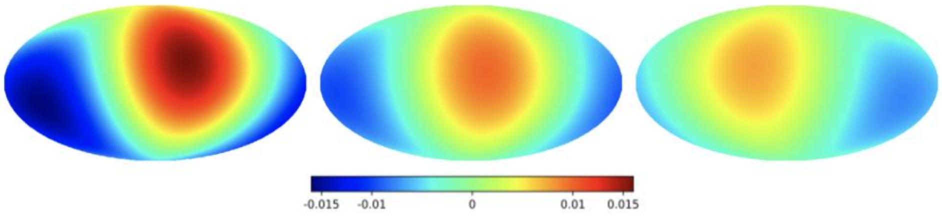

60%

45%

Conclusion

- Designed a new observable measuring the expansion rate fluctuations and determine its multipoles.

- A simple dipole term is a poor representation of the angular fluctuations in the local expansion rate.

- Find a signal for the quadrupolar component for both galaxies and SNIa of the CF3 sample.

- The maximum of the quadrupole is aligned with dipole, and it is axially symmetric.

- The octupole (from galaxy sample only) has a maximum in the direction of the dipole.

- Need to build on the current work with updated and enlarged datasets: CosmicFlows-4, Pantheon+.

Spherical Harmonic analysis : parameters

Sample	N_{pix}	l_d	b_d	$\hat{C}_1$ (10^{-4})	$\frac{\eta_{1max}-\lvert\eta_{1min}\rvert}{2}$ (10^{-2})	p-value (%)	l_q	b_q	$\hat{C}_2$ (10^{-4})	$\frac{\eta_{2max}-\lvert\eta_{2min}\rvert}{2}$ (10^{-2})	p-value (%)	l_t	b_t	$\hat{C}_3$ (10^{-4})	$\frac{\eta_{3max}-\lvert\eta_{3min}\rvert}{2}$ (10^{-2})	p-value (%)
CF3 [0.01, 0.05]	192	291 ± 15	12 ± 7	3.0 ± 1.6	1.6	0.03	323 ± 16	9 ± 4	2.4 ± 0.9	1.9	0.12	289 ± 24	16 ± 15	0.1 ± 0.4	1.2	30.44
CF3 [0.01, 0.05]	48	283 ± 6	12 ± 5	5.3 ± 0.8	1.9	< 0.01	310 ± 11	4 ± 8	0.9 ± 0.3	1.1	< 0.01	284 ± 7	12 ± 5	0.5 ± 0.2	1.3	0.01
CF3g [0.01, 0.05]	48	286 ± 7	4 ± 6	7.0 ± 1.0	2.0	< 0.01	338 ± 8	22 ± 5	1.1 ± 0.4	1.3	< 0.01	255 ± 9	11 ± 5	0.7 ± 0.2	1.5	0.01
CF3 [0.01, 0.05]	12	285 ± 5	11 ± 4	5.1 ± 0.8	1.9	< 0.01	308 ± 7	1 ± 7	1 ± 0.3	1.1	< 0.01	-	-	-	-	-
CF3g [0.01, 0.05]	12	296 ± 6	18 ± 5	4.0 ± 0.6	1.7	< 0.01	323 ± 34	2 ± 17	1.3 ± 0.4	1.4	< 0.01	-	-	-	-	-
CF3sn [0.01, 0.05]	12	322 ± 23	-8 ± 18	3.7 ± 1.5	1.5	0.27	343 ± 15	-8 ± 10	1.7 ± 1.4	1.7	2.90	-	-	-	-	-
Pantheon [0.01, 0.05]	12	334 ± 42	6 ± 20	3.5 ± 2.7	1.6	4.37	337	-5	0.6 ± 1.9	1.6	33.33	-	-	-	-	-
CF3 [0.01, 0.03]	12	279 ± 5	12 ± 5	7.8 ± 1.0	2.3	< 0.01	310 ± 8	11 ± 6	2.9 ± 0.6	1.9	< 0.01	-	-	-	-	-
CF3 [0.03, 0.05]	12	301 ± 15	10 ± 14	1.1 ± 0.7	1.0	0.03	277 ± 28	-12 ± 11	0.9 ± 0.3	1.0	2.04	-	-	-	-	-